Article

Temperature Dependence of Domain Motions of Calmodulin Probed by NMR Relaxation at Multiple Fields

Shou-Lin Chang, Attila Szabo, and Nico Tjandra

J. Am. Chem. Soc., **2003**, 125 (37), 11379-11384• DOI: 10.1021/ja034064w • Publication Date (Web): 22 August 2003

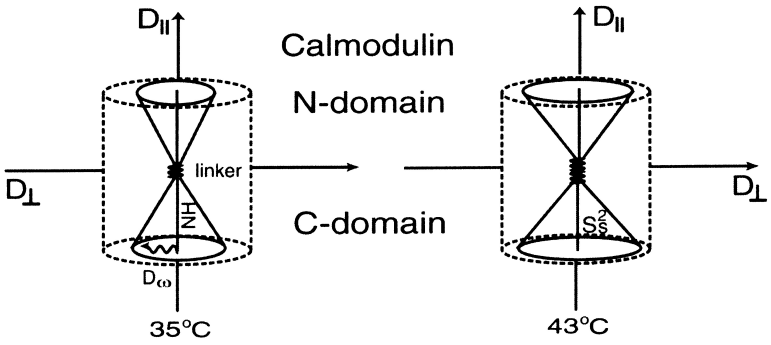

More About This Article

Additional resources and features associated with this article are available within the HTML version:

- Supporting Information
- Links to the 4 articles that cite this article, as of the time of this article download
- Access to high resolution figures
- Links to articles and content related to this article
- Copyright permission to reproduce figures and/or text from this article

View the Full Text HTML

Journal of the American Chemical Society is published by the American Chemical Society. 1155 Sixteenth Street N.W., Washington, DC 20036

J|A|C|S
ARTICLES
Published on Web 08/22/2003

Temperature Dependence of Domain Motions of Calmodulin Probed by NMR Relaxation at Multiple Fields

Shou-Lin Chang,[†] Attila Szabo,[‡] and Nico Tjandra*[,†]

Contribution from the Laboratory of Biophysical Chemistry, Building 50, National Heart, Lung, and Blood Institute and Laboratory of Chemical Physics, National Institute of Diabetes, Digestive and Kidney Diseases, National Institutes of Health, Bethesda, Maryland 20892

Received January 7, 2003; E-mail: nico@helix.nih.gov

Abstract: Interdomain motions of Ca^{2+}-ligated calmodulin were characterized by analyzing the nuclear magnetic resonance ^{15}N longitudinal relaxation rate R_1, transverse relaxation rate R_2, and steady-state $\{^1H\}-^{15}N$ NOE of the backbone amide group at three different magnetic field strengths (18.8, 14.1, and 8.5 T) and four different temperatures (21, 27, 35, and 43 °C). Between 35 and 43 °C, a larger than expected change in the amplitude and the time scale of the interdomain motion for both N- and C-domains was observed. We attribute this to the shift in population of four residues (74−77) in the central linker from predominantly helical to random coil in this temperature range. This is consistent with the conformation of these residues in the calmodulin−peptide complex, where they are nonhelical. The doubling of the disordered region of the central helix (residues 78−81 at room temperature) when temperature is raised from 35 to 43 °C results in larger amplitude interdomain motion. Our analysis of the NMR relaxation data quantifies subtle changes in the interdomain dynamics and provides an additional tool to monitor conformational changes in multidomain proteins.

Introduction

Calmodulin (CaM) is a calcium-sensing protein that is highly conserved across the eukaryotes.[1] It participates in numerous Ca^{2+}-dependent cellular regulatory processes that lead to important physiological events including proliferation, motility, and cell cycle progression. Calmodulin has four calcium-binding sites formed by a helix−loop−helix motif, known as EF hands [2]. The X-ray structure of Xenopus CaM [3] reveals a dumbbell-shaped molecule consisting of two globular domains connected by a long central helix. In the crystal structure, the two domains are in a trans-like orientation. Early studies by small-angle X-ray scattering [4] and NMR relaxation [5] indicated that the central helix is flexible. The central helix has also been shown to have temperature-dependent conformational variability in the crystalline environment.[6] This flexibility plays a crucial role for the function of CaM.[7] It dynamically modulates the relative distance and orientation of the two domains upon calcium and ligand binding. This allows CaM to adopt various conformations to fit and interact with a broad spectrum of targets.

Calmodulin is one of many multidomain proteins for which the relative orientation of different domains is important for their physiological function. In solution, domain orientation can be readily extracted from residual dipolar couplings by preparing protein samples in alignment media.[8−10] This assumes that the relative domain orientation is fixed or one average conformation can represent the dynamic population of the domains. When the domain orientation is dynamic, its behavior can be characterized by careful analysis of NMR relaxation data.[11,12] Previously, we have shown that calmodulin tumbles anisotropically. The overall rotational diffusion of this protein was best described by an axially symmetric model. In addition, we have determined that each domain within calmodulin undergoes independent diffusion at a faster rate than the overall tumbling of the protein. The interdomain motion of each domain was characterized by an order parameter and a time constant on the nanosecond time scale. In this work, we probe the interdomain motion of Ca^{2+}-CaM at several different temperatures using NMR relaxation data from multiple fields. The study of the temperature dependence of the amplitude and time scale of slow interdomain motions can in principle provide us with the information about the nature of the central helix that links the two domains.

[†] Laboratory of Biophysical Chemistry, National Heart, Lung, and Blood Institute, National Institutes of Health.

[‡] Laboratory of Chemical Physics, National Institute of Diabetes, Digestive and Kidney Diseases, National Institutes of Health.

(1) Cohen, P.; Klee, C. B. *Calmodulin*; Elsevier: 1988.
(2) Kretsinger, R. H.; Nockolds, C. E. *J. Biol. Chem.* **1973**, *248*, 3313−3326.
(3) Babu, Y. S.; Bugg, C. E.; Cook, W. J. *J. Mol. Biol.* **1988**, *204*, 191−204.
(4) Seaton, B. A.; Head, J. F.; Engelman, D. M.; Richards, F. M. *Biochemistry* **1985**, *24*, 6740−6743.
(5) Barbato, G.; Ikura, M.; Kay, L. E.; Pastor, R. W.; Bax, A. *Biochemistry* **1992**, *31*, 5269−5278.
(6) Wilson, M. A.; Brunger, A. T. *J. Mol. Biol.* **2000**, *301*, 1237−1256.
(7) Crivici, A.; Ikura, M. *Annu. Rev. Biophys. Biomol. Struct.* **1995**, *24*, 85−116.
(8) Tjandra, N.; Bax, A. *Science* **1997**, *278*, 1111−1114.
(9) Goto, N. K.; Skrynnikov, N. R.; Dahlquist, F. W.; Kay, L. E. *J. Mol. Biol.* **2001**, *308*, 745−764.
(10) Fischer, M. W.; Losonczi, J. A.; Weaver, J. L.; Prestegard, J. H. *Biochemistry* **1999**, *38*, 9013−9022.
(11) Chang, S. L.; Tjandra, N. *J. Am. Chem. Soc.* **2001**, *123*, 11484−11485.
(12) Baber, J. L.; Szabo, A.; Tjandra, N. *J. Am. Chem. Soc.* **2001**, *123*, 3953−3959.

Material and Method

NMR Spectroscopy. The preparation of the *Xenopus* calmodulin sample for NMR relaxation studies was described previously.[13,14] The 220 μL NMR sample contained 1.6 mM uniformly ^{15}N-labeled calmodulin, 8.0 mM $CaCl_2$, 100 mM KCl, 100 μM NaN_3, and 5% D_2O at pH 6.36. NMR experiments at 21, 27, 35, and 43 °C were performed on Bruker DMX 360, DMX 600, and DRX 800 spectrometers. All spectrometers were equipped with a shielded *x,y,z*-pulsed field gradient triple resonance 5 mm probe. States-TPPI quadrature detection in t_1 dimension was used for all experiments. ^{15}N and ^{1}H carrier frequencies were set to 116.5 ppm and water frequency, respectively. NMR data were processed using NMRPipe [15] and analyzed with PIPP software.[16]

The standard T_1 and $T_{1\rho}$ pulse sequences [17] were modified to include WATERGATE [18] solvent suppression, pulsed-field gradients, and a semiconstant time evolution period in t_1.[19] ^{15}N continuous spin-locking at 2500 Hz was used for all $T_{1\rho}$ experiments. To minimize the effects of sample heating or changes in NMR condition, $T_{1\rho}$ data were collected in an interleaved fashion. Eight relaxation delays per experiment were randomly chosen in a way such that a 90% drop in intensity was obtained going from the shortest to longest delay. Relaxation times were determined by fitting the delay dependent peak intensities to an exponential function using the Powell nonlinear optimization or Levenberg−Marquardt method.[20] T_2 values were calculated from the corresponding $T_{1\rho}$, T_1, chemical shift values, spin-lock field strength, and ^{15}N carrier frequency. Error estimation was done by using 300 Monte Carlo simulations.[20]

The NOE pulse sequence with water flip-back described by Grzesiek and Bax[21] was used for all $\{^1H\}-^{15}N$ NOE measurements. NOE values were calculated by taking the ratio of peak intensities from experiments performed with and without ^{1}H presaturation. The proton frequency was shifted off-resonance by about 3 MHz during the presaturation period for the unsaturated measurements. Saturated and unsaturated spectra were acquired in an interleaved manner. The pulse train used for ^{1}H saturation utilized 162 pulses separated by 50 ms delays and was applied for a total of 2.2, 2.2, and 3.8 s in the 360, 600, and 800 MHz experiments, respectively.

Dynamics Analysis of Domain Motions. The relaxation rates are functions of the spectral density of molecular motion. Relaxation rates ^{15}N R_1, R_2 and $\{^1H\}-^{15}N$ NOE for an N−H interaction vector can be expressed as

$$R_1 = d^2[J(w_H - w_N) + 3J(w_N) + 6J(w_H + w_N)] + c^2J(w_N)$$

$$R_2 = \frac{1}{2}d^2[4J(0) + J(w_H - w_N) + 3J(w_N) + 6J(w_H) + 6J(w_H + w_N)] + \frac{1}{6}c^2[3J(w_N) + 4J(0)]$$

$$\mathrm{NOE} = 1 + \frac{\gamma_H}{\gamma_N}d^2[6J(w_H + w_N) - J(w_H - w_N)]\frac{1}{R_1} \qquad (1)$$

where $d^2 = (^1/_{10})[(\gamma_H\gamma_N h)/(2\pi r^3_{NH})]^2$, $c^2 = (^2/_{15})[\omega^2_N(\sigma_{||} - \sigma_\perp)^2]$, h is Planck's constant, r_{NH} is the internuclear N−H distance (0.102 nm), γ_i is the gyromagnetic ratio of spin I, and $\sigma_{||}$, $\sigma_\perp$ are components of the axially symmetric ^{15}N chemical shift anisotropy tensor. The value for $(\sigma_{||} - \sigma_\perp)$ is −172 ppm as reported,[22−24] and the unique axis is assumed to align in the same direction as the N−H vector. The form of spectral density depends on the type of motion the NH bond vector experiences. For a molecule that undergoes an axially symmetric overall tumbling and has internal motions on two distinct time scales, where the slower time scale is for describing domain motion, the Liparid−Szabo approach was used as described previously. The $J(w)$ has the form

$$J(w) = \sum_{k=1}^{3} A_k\{ S_f^2S_s^2[\tau_k/(1 + w^2\tau_k^2)] + S_f^2(1 - S_s^2)[\tau_{s,k}/(1 + w^2\tau_{s,k}^2)] + (1 - S_f^2)[\tau_{f,k}/(1 + w^2\tau_{f,k}^2)]\}$$

with,

$$A_1 = 0.75\sin^4\alpha,\ A_2 = 3(\sin^2\alpha)(\cos^2\alpha),\ A_3 = (1.5\cos^2\alpha - 0.5)^2$$

$$\tau_1 = (4D_{||} + 2D_\perp)^{-1}, \tau_2 = (D_{||} + 5D_\perp)^{-1}, \tau_3 = (6D_\perp)^{-1}$$

$$1/\tau_{i,k} = 1/\tau_i + 1/\tau_k;\ i = \mathrm{s,f\ and}\ k = 1,2,3 \qquad (2)$$

where α is the angle between the N−H bond vector and the unique axis of the rotational diffusion tensor and $D_{||}$ and $D_\perp$ are the parallel and perpendicular components of the diffusion tensor for the global tumbling, respectively. An effective overall correlation time for axially symmetric tumbling here is defined as $\tau_c = (2D_{||} + 4D_\perp)^{-1}$. The slower time constant τ_s and its associated order parameter S_s^2 in the extended Lipari−Szabo approach are used to describe the interdomain motion. Here, residues within the same protein domain are assumed to experience the same domain motion, that is, with the same amplitude and time constant. The fast internal motion parameters τ_f and S_f^2 describe the local motion of the N−H vector. Further simplification can be made if we exclude residues that undergo large amplitude motion or exhibit conformational exchange from analysis. Under such circumstance, an average τ_f and S_f^2 is used for all the N−H vectors within the same domain to simplify the optimization procedures. The criteria for such exclusion are for residues with

$$\mathrm{NOE} < 0.4 \qquad (1)$$

$$\mathrm{NOE} < \langle\mathrm{NOE}\rangle - 1.0*\langle\mathrm{NOE}\rangle_{SD} \qquad (2)$$

$$T_2 < \langle T_2\rangle - 1.0*\langle T_2\rangle_{SD} \text{ and } (\langle T_2\rangle - T_2)/\langle T_2\rangle > 3.0*(T_1 - \langle T_1\rangle)/\langle T_1\rangle$$

where "⟨⟩" and "⟨⟩$_{SD}$" stand for the average value and the standard deviation of the corresponding physical quantity in the angle brackets.

Minimization and Fitting of Experimental Data. Once those residues with motions significantly different from the bulk are excluded, NMR relaxation data were fitted by minimizing the target error function E:

$$E = \sum_{i,j,k,l} (R^e_{i,j,k,l} - R^c_{i,j,k,l})^2/\sigma^2_{i,j,k,l} \qquad (3)$$

where $R^e_{i,j,k,l}$, $R^c_{i,j,k,l}$, and $\sigma_{i,j,k,l}$ are the experimental and theoretically calculated relaxation data and the standard deviation of relaxation data i (R_1, R_2, or NOE) at field j for residue k at temperature l. The effective overall tumbling correlation times are constrained with the Stokes−Einstein equation,

$$\tau_c = \eta V/kT \qquad (4)$$

in which η is the solvent's viscosity, k is the Boltzmann constant, T is the temperature in Kelvin, and V is the solvated volume of the rotating molecule. All datasets from four different temperatures are minimized

(13) Tjandra, N.; Kuboniwa, H.; Ren, H.; Bax, A. *Eur. J. Biochem.* **1995**, *230*, 1014−1024.
(14) Ikura, M.; Clore, G. M.; Gronenborn, A. M.; Zhu, G.; Klee, C. B.; Bax, A. *Science* **1992**, *256*, 632−638.
(15) Delaglio, F.; Grzesiek, S.; Vuister, G. W.; Zhu, G.; Pfeifer, J.; Bax, A. *J. Biomol. NMR* **1995**, *6*, 277−293.
(16) Garrett, D. S.; Powers, R.; Gronenborn, A. M.; Clore, G. M. *J Magn Reson* **1991**, *95*, 214−220.
(17) Kay, L. E.; Torchia, D. A.; Bax, A. *Biochemistry* **1989**, *28*, 8972−8979.
(18) Piotto, M.; Saudek, V.; Sklenar, V. *J. Biomol. NMR* **1992**, *2*, 661−665.
(19) Grzesiek, S.; Bax, A. *J. Biomol. NMR* **1993**, *3*, 185−204.
(20) Press, W. H.; Teukolsky, S. A.; Vetterling, W. T.; Flannery, B. P. *Numerical Recipes in C*, 2nd ed.; Cambridge University Press: Cambridge, 1999.
(21) Grzesiek, S.; Bax, A. *J. Am. Chem. Soc.* **1993**, *115*, 12593−12594.
(22) Boyd, J.; Redfield, C. *J. Am. Chem. Soc.* **1999**, *121*, 7441−7442.
(23) Kroenke, C. D.; Rance, M.; Palmer, A. G. *J. Am. Chem. Soc.* **1999**, *121*, 10119−10125.
(24) Lee, A. L.; Wand, A. J. *J. Biomol. NMR* **1999**, *13*, 101−112.

simultaneously with a total of 53 variables. One of these, when scaled by the viscosity, determines the overall tumbling correlation times. The rest describe the domain and fast motion of the N- and C-domain at each temperature. Error estimation was achieved by using 200 Monte Carlo simulations. The synthetic data sets were generated by adding random errors to the experimental data. The random errors were normally distributed with mean zero and variance equal to the estimated experimental standard deviation. The resulting error bars for the parameters turned out to be suspiciously small, consequently, the statistical significance of the number of parameters used in the fitting procedure was evaluated using reduced error analysis.[25,26]

Reduced Error Analysis. In general, the fit between a model and experimental data improves with the number of adjustable parameters. We need to determine whether the reduction in the error function found by introducing different fitting parameters at different temperatures is statistically significant. To serve this purpose, the so-called reduced error function [25,26] is defined as $E_v(m) = E(m)/(N - m)$, where N is the number of independently measured variables (here the total relaxation times measured), m is the number of variables used in the fitting procedure, and $E(m)$ is the resulting error as defined in eq 3. If two fitting procedures with m and $m + k$ variable parameters are performed, a test for the validity of adding k terms can be carried out by calculating the ratio $F = [E(m) - E(m + k)]/[kE_v(m + k)]$.[25] A large F value justifies the inclusion of the additional terms in the fit. A more stringent measure involves the integral function, $P_F(F; k, N - m - k)$, which represents the probability that the observed improvement in the $(m + k)$ parameter fit over the m parameter fit is obtained by chance. Typically P_F values that are smaller than 0.01 are considered to be statistically significant. To be conservative in evaluating our fitting results, we use 0.001 as a cutoff to determine whether the inclusion of more fitting parameters is statistically significant.

Dynamics Analysis of "Parallel Residues". Backbone N−H vectors that are parallel to the unique rotational diffusion axis $D_{||}$ sense only motions perpendicular to the $D_{||}$ axis. In the case of Ca^{2+}-ligated calmodulin, the central helix contains these "parallel residues" (residues from 65 to 77 and 82 to 90). They can be identified with their large T_1/T_2 ratio.[12] These "parallel residues" are good sensors for probing the "bending" and are insensitive to the "twisting" type of domain motion. The dynamical analysis of "parallel residues" is similar to the methodology described above for domain motion.

Relationship between the Effective Correlation Time and Diffusion Constant in the Wobble-in-a-Cone Model. For the diffusion in the cone model, the relationship between the semicone angle β, diffusion coefficient D_ω, the order parameter S_{cone}, and effective correlation time τ_s is given by the equation[27]

$$D_\omega(1 - S_{cone}^2)\tau_s = x^2(1 + x)^2\{\ln[(1 + x)/2] + (1 - x)/2\}/[2(x - 1)] + (1 - x)(6 + 8x - x^2 - 12x^3 - 7x^4)/24$$

$$\text{with } S_{cone} = \frac{1}{2}x(1 + x)$$

$$\text{and } x = \cos(\beta) \qquad (5)$$

Result

Initial Analysis. NMR relaxation data T_1, T_2, and NOE of Ca^{2+}-CaM at 21, 27, 35, and 43 °C for three different magnetic fields 18.8, 14.1, and 8.5 T (Figure 1 shows the temperature dependence of relaxation data at 18.8 T, and Figure 2 shows the field dependence of relaxation data at 35 °C) were fitted using eqs 1, 2, and 4 by minimizing the target error function E, given in eq 3. The average percentage errors were as follows: 1.6 (T_1, 800 MHz), 1.2 (T_1, 600 MHz), 3.8 (T_1, 360 MHz), 1.8

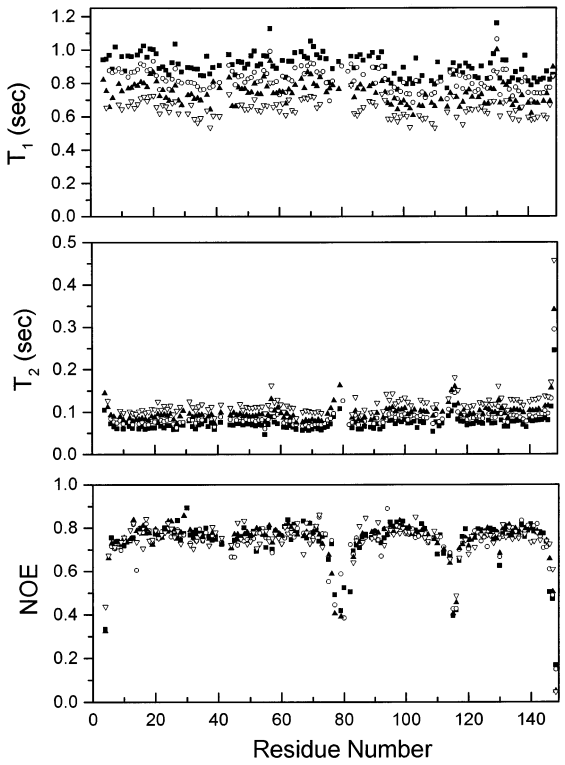

Figure 1. ^{15}N relaxation data of Ca^{2+}-calmodulin at 18.8 T. Squares, circles, up triangles, and down triangles represent data at 21, 27, 35, and 43 °C, respectively. (a) Longitudinal relaxation time T_1, (b) transverse relaxation T_2, (c) steady-state $\{^1H\}^{15}N$ NOE.

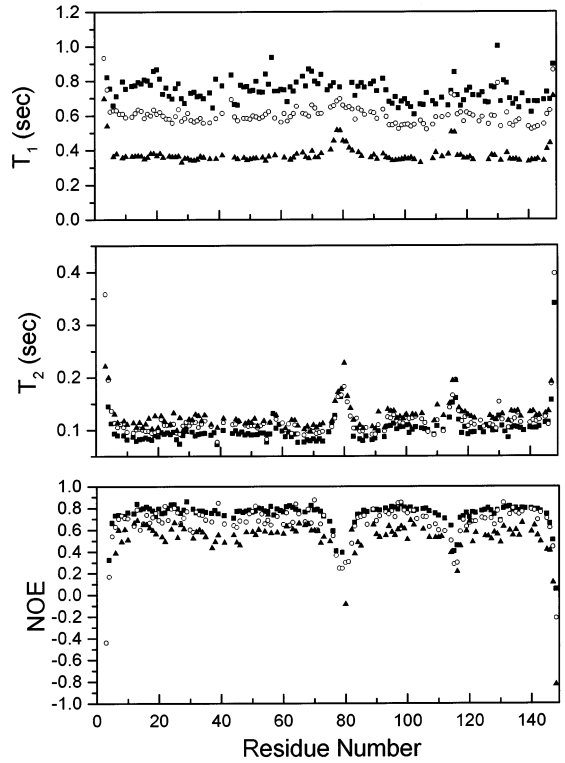

Figure 2. ^{15}N relaxation data of Ca^{2+}-calmodulin at 35 °C. Squares, circles, and up triangles represent data at spectrometer frequency 800, 600, and 360 MHz, respectively. (a) Longitudinal relaxation time T_1, (b) transverse relaxation T_2, (c) steady-state $\{^1H\}^{15}N$ NOE.

(25) Bevington, P. R.; Robinson, D. K. *Data reduction and error analysis for the physical sciences*, 2nd ed. McGraw-Hill: New York, NY, 1992.
(26) Tjandra, N.; Wingfield, P.; Stahl, S.; Bax, A. *J. Biomol. NMR* **1996**, *8*, 273−284.
(27) Lipari, G.; Szabo, A. *Biophys. J.* **1980**, *30*, 489−506.

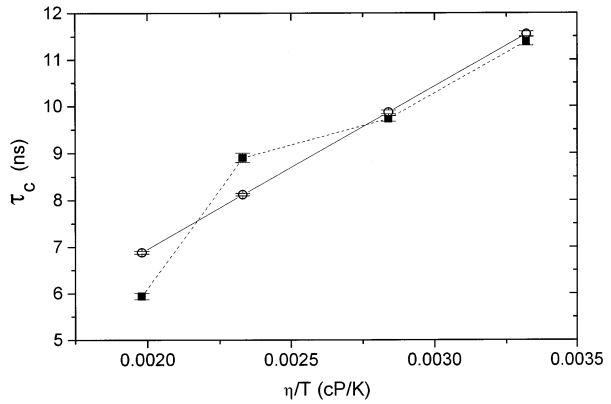

Figure 3. Optimized effective overall correlation times. Open circles represent the values obtained from fitting data sets at 21, 27, 35, and 43 °C simultaneously by imposing Stokes−Einstein equation on the effective overall diffusion rate. Solid squares are values calculated by treating data set at each temperature separately.

(T_2, 800 MHz), 2.7 (T_2, 600 MHz), 7.4 (T_2, 360 MHz), 4.9 (NOE, 800 MHz), 6.1 (NOE, 600 MHz), and 8.6 (NOE, 360 MHz) at 21 °C; 1.7 (T_1, 800 MHz), 3.2 (T_1, 600 MHz), 3.6 (T_1, 360 MHz), 1.3 (T_2, 800 MHz), 2.3 (T_2, 600 MHz), 4.2 (T_2, 360 MHz), 3.2 (NOE, 800 MHz), 5.3 (NOE, 600 MHz), and 8.2 (NOE, 360 MHz) at 27 °C; 2.1 (T_1, 800 MHz), 3.4 (T_1, 600 MHz), 2.0 (T_1, 360 MHz), 1.4 (T_2, 800 MHz), 2.4 (T_2, 600 MHz), 5.3 (T_2, 360 MHz), 1.3 (NOE, 800 MHz), 5.1 (NOE, 600 MHz), and 8.4 (NOE, 360 MHz) at 35 °C; 2.7 (T_1, 800 MHz), 3.1 (T_1, 600 MHz), 4.6 (T_1, 360 MHz), 2.5 (T_2, 800 MHz), 3.3 (T_2, 600 MHz), 4.8 (T_2, 360 MHz), 5.5 (NOE, 800 MHz), 6.0 (NOE, 600 MHz), and 13.0 (NOE, 360 MHz) at 43 °C. Residues from 1 to 77 are classified as N-domain residues, and 82 to 148, as C-domain residues. The optimized effective overall correlation times are 11.39, 9.73, 8.85, and 5.94 ns (Figure 3) at 21, 27, 35, and 43 °C, respectively. However, we noticed that at the higher temperatures the optimization results in a very shallow error function surface along parameters τ_c and τ_s, and thus these cannot be found uniquely. To circumvent this, we used the Stokes−Einstein equation to constrain the parameters describing overall tumbling and to obtain a more reliable estimate of the time scale of slow domain motions. The viscosity of water is used throughout the calculations. The fitting results are given in Table 1. Standard deviations of the fitted parameters were estimated using a Monte Carlo approach. We found the standard deviation to be small. However, this method does not take into account the possible shallowness of the minimum which can lead to large correlations among the values of the parameters. A more reliable evaluation of statistical significance of the fitted parameters can be obtained using reduced error analysis.

Statistical Significance of the Temperature Dependence. To check the dependence between 21 and 35 °C, we systematically removed the temperature dependence of each parameter separately and used only one instead of three fitting variables for three temperatures for the rotational diffusion anisotropy ($D_\parallel/D_\perp$), the orientation of diffusion axis with respect to molecular frame θ and φ, the fast motion parameters τ_f and S_f^2, and slow interdomain motion parameters τ_s and S_s^2. The only dependence we found to be statistically significant is that of S_s^2 (F, $P_F = 9.76$, 6.06×10^{-5} for N-domain and 9.22, 1.03×10^{-4} for C-domain). The rest of the parameters such as fast motion parameters and the angles θ and ϕ have no significant temperature dependence ($P_F > 0.001$). Using the same procedure, we examined the fits from 21 to 43 °C. Again, the trend of the slow motion order parameters is statistically significant (F, $P_F = 35.92$, 9.28×10^{-23} for N-domain and 64.90, 1.62×10^{-40} for C-domain). In addition, the dependence of slow motion correlation times τ_s is also significant (F, P_F=7.27, 7.40×10^{-5} for N-domain and 6.78, 1.50×10^{-4} for C-domain). This indicates the trend of slow motion time constants from 21 to 35 °C is not significant, but its sudden increase from 35 to 43 °C is significant. Consequently, we did a final fit by removing the temperature dependence of $D_\parallel/D_\perp$, θ, φ, τ_f, and S_f^2 from 21 to 43 °C and using only one τ_s for temperature from 21 to 35 °C. This is the maximum number of parameters that can reliably be extracted from the experimental data. The results are given in Table 2, and the temperature dependence of the parameters describing slow interdomain motion is shown in Figure 4. The effective overall tumbling correlation times are 11.55, 9.87, 8.12, and 6.88 at 21, 27, 35, and 43 °C, respectively (Figure 3). The slow correlation time for the N-domain is 2.47 ns from 21 to 35 °C and changes to 3.29 at 43 °C, and for the C-domain, the correlation time is 2.95 ns from 21 to 35 °C and increases to 4.26 at 43 °C. The slow interdomain motion order parameter drops from 0.79 to 0.77, 0.77, and 0.68 from 21 to 43 °C for the N-domain, and for the C-domain, it decreases from 0.72 to 0.70, 0.68, and 0.53. The order parameter of the C-domain at 43 °C corresponds to a semicone angle of 36°. To ascertain whether this value is not physically unreasonable, we carried out rigid body rotations of the N-domain about an axis passing through the center and oriented perpendicular to the central helix, keeping the C-domain fixed. The rotation was stopped when any atom in one domain is within 2.5 Å away from the other domain. The N-domain was then twisted in a 15° increment, and the same rotation was performed. Finally, the rotation axis was moved about the central helix in a 15° increment, and the bending and twisting procedures were repeated. The smallest maximum angular excursion of 160° was obtained. For a symmetric system, this corresponds to an allowed semicone angle of 40°.

Discussion

In this paper, we have analyzed the backbone ^{15}N NMR relaxation parameters T_1, T_2, and NOE at 21, 27, 35, and 43 °C and at 18.8, 14.1, and 8.5 T of calmodulin. Our key result is the significant drop in the slow order parameter from 35 to 43 °C, indicating an unexpected increase in the amplitude of interdomain motions. The simplest explanation is that the flexibility of the central helix increases. Specifically we suggest that the disordered region of the central helix (residues 78−81) doubles in size on going from 35 to 43 °C because residues 74−77 partially "melt". The implied relatively low propensity of residues 74−77 for the helical conformation is consistent with the fact that when calmodulin is complexed with its target peptide, not only residues 78−81 but also residues 74−77 adopt nonhelical conformations.[5,7,14] The fact that the resonances of residues 74−81 in the HSQC spectrum have disappeared at 43 °C implies the existence of an exchange process on the microsecond−millisecond time scale. Thus it is possible that at this temperature there are at least two calmodulin populations with different conformations of the central helix that interconvert on the microsecond−millisecond time scale. Since our analysis

Table 1. Dynamical Parameters of Ca^{2+}-CaM Derived from NMR Relaxation Data (Data at Four Temperatures and Three Fields Were Fitted Simultaneously Using Extended Lipari−Szabo Approach and Imposing Stokes Equation on the Overall Tumbling)

	21 °C		27 °C		35 °C		43 °C	
	N	C	N	C	N	C	N	C
τ_c (ns)	11.86 ± 0.02		10.13 ± 0.02		8.33 ± 0.01		7.06 ± 0.01	
$D_\parallel/D_\perp$	1.64 ± 0.02		1.66 ± 0.02		1.61 ± 0.02		1.70 ± 0.03	
θ (deg)	68 ± 1	69 ± 1	69 ± 1	67 ± 1	67 ± 1	64 ± 1	70 ± 2	58 ± 2
ϕ (deg)	98 ± 1	149 ± 1	91 ± 1	145 ± 1	93 ± 1	141 ± 1	89 ± 1	139 ± 2
τ_s (ns)	2.4 ± 0.1	2.7 ± 0.1	2.9 ± 0.1	3.2 ± 0.1	2.5 ± 0.1	3.1 ± 0.1	4.5 ± 0.3	4.6 ± 0.1
S_s^2	0.77 ± 0.002	0.70 ± 0.002	0.75 ± 0.003	0.68 ± 0.002	0.75 ± 0.003	0.66 ± 0.003	0.62 ± 0.009	0.50 ± 0.008
τ_f (ps)	9 ± 2	8 ± 1	14 ± 1	16 ± 1	14 ± 1	16 ± 1	27 ± 2	22 ± 2
S_f^2	0.86 ± 0.002	0.84 ± 0.002	0.86 ± 0.002	0.84 ± 0.001	0.87 ± 0.003	0.85 ± 0.002	0.85 ± 0.002	0.84 ± 0.002

Table 2. . Dynamical Parameters of Ca^{2+}-CaM Derived from NMR Relaxation Data (Data at Four Temperatures and Three Fields Were Fitted Simultaneously Using Extended Lipari−Szabo Approach with a Maximum Set of Variables that Satisfy the Experimental Data)

	21 °C		27 °C		35 °C		43 °C	
	N	C	N	C	N	C	N	C
τ_c (ns)	11.55		9.87		8.12		6.88	
$D_\parallel/D_\perp$	1.62		1.62		1.62		1.62	
θ (deg)	69	67	69	67	69	67	69	67
ϕ (deg)	94	146	94	146	94	146	94	146
τ_s (ns)	2.47	2.95	2.47	2.95	2.47	2.95	3.3	4.3
S_s^2	0.79	0.72	0.77	0.70	0.77	0.68	0.68	0.53
D_ω (ns^{-1})	0.017	0.020	0.019	0.021	0.019	0.023	0.020	0.024
τ_f (ps)	14	15	14	15	14	15	14	15
S_f^2	0.87	0.85	0.87	0.85	0.87	0.85	0.87	0.85

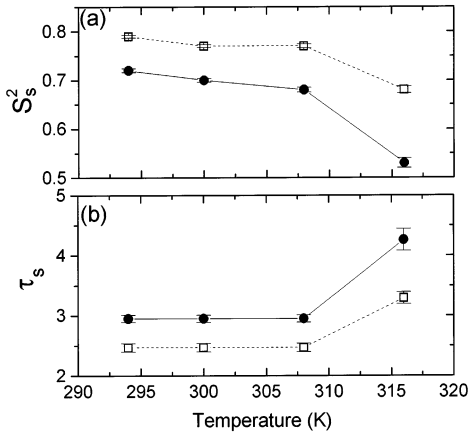

Figure 4. Slow interdomain motional parameters for calmodulin. Open squares and solid circles represent data for N- and C-domain, respectively. (a) Order parameters, (b) correlation times.

assumed a single conformation at 43 °C, the resulting order parameters are likely to be effective ones.

Similar to the interdomain order parameter, an abrupt increase in slow correlation time is observed. The fact that the correlation time for slow interdomain motion actually increases between 35 and 43 °C might at first sight seem inconsistent with increased flexibility. However, it must be remembered that τ_s is an effective correlation time that depends on both the amplitude and "rate" of the motion. Specifically if, within the framework of the cone model, S_s^2 and τ_s are used to obtain the diffusion coefficient describing interdomain motion, this diffusion coefficient does indeed increase with increasing temperature as shown in Figure 5. Thus the dramatic change of τ_s from 35 to 43 °C is due to the drop of the order parameter or increase in the β angle value. For a fixed diffusion coefficient, the

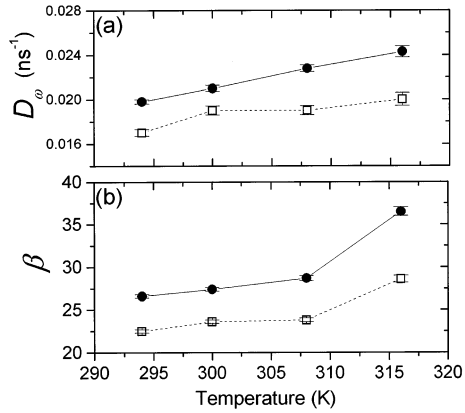

Figure 5. Slow interdomain motional parameters for calmodulin assuming wobble-in-a-cone model. Open squares and solid circles represent data for N- and C-domain, respectively. (a) Diffusion coefficients in the cone, (b) semicone angles.

effective correlation times increase when the order parameter is lowered. Qualitatively, this is a reflection of the fact that the more restricted the motion, the shorter the time required for the N- or C-domain, viewed as rigid bodies, to explore the available conformational space.

The order parameters and effective correlation times that describe the motion of the N- and C-domain are somewhat different. This is not unexpected since the molecule is asymmetric. However, it is not straightforward to provide quantitative explanations for the differences. Consider, for example, the fact that τ_s is smaller for the N-domain. At first sight, this appears inconsistent with the fact that the N-domain has more amino acids and has a larger volume. However, as described above, both the amplitude and the rotational rate contribute to the effective correlation time. Indeed, as shown in Figure 5, D_ω for the N-domain is smaller.

The N−H bond vectors of "parallel residues" (residue 65−74 on the N-domain and 82−90 on the C-domain) point along the helix axis and are insensitive to rotations about this axis. Using the same approach as that used for "domain residues", we analyzed the dynamics of the "parallel residues". Since these N−H vectors will sense only the perpendicular component of the overall tumbling, the overall correlation time we obtain for the "parallel residues" should correspond to $1/(6D_\perp)$ of the overall tumbling for the whole molecule. Indeed, the fitted correlation time is within 5% of the $1/(6D_\perp)$ value of the "domain residues". The calculated order parameters S_{para}^2 for the N-domain (0.80, 0.79, 0.78, and 0.70 at 21, 27, 35, and 43 °C, respectively) are essentially the same as the corresponding S_s^2 values for the "domain residues". However, the S_{para}^2 values

for the C-domain (0.77, 0.76, 0.76 and 0.59 at 21, 27, 35, and 43 °C, respectively) are higher than those of the "domain residues" indicating that the C-domain can undergo a twisting motion about the helix axis.

Traditionally, the thermostability of calmodulin has been studied using scanning microcalorimetry and circular dichroism (CD) in the far and near UV regions. Virtually all previous studies using such conventional techniques showed that Ca^{2+}-calmodulin is thermodynamically stable up to 90 °C or in the presence of high concentration denaturation reagents such as urea and guanidine hydrochloride without indication of unfolding of the central helix or the two domains.[28−30] A notable exception is the CD data from Martin et al. (1986) which showed a subtle transition occurring between 35 °C and 45 °C.[31] These authors had no clear explanation for this, and it is tempting to suggest that it was due to the same physical process that we described here. In this study, by analyzing NMR relaxation data at multiple fields, we found that the amplitude and correlation time of interdomain motion had an unexpected temperature dependence. We attributed this to a transition from helix to coil states of a few residues of the central helix linker. The sensitivity of NMR relaxation to such subtle changes suggests that this type of analysis should prove useful in the study of other multidomain proteins.

Supporting Information Available: ^{15}N relaxation data for calmodulin at three fields (18.8, 14.1, and 8.5 T) and four temperatures (21, 27, 35, and 43 °C). This material is available free of charge via the Internet at http://pubs.acs.org.

JA034064W

(28) Brzeska, H.; Venyaminov, S.; Grabarek, Z.; Drabikowski, W. *FEBS Lett.* **1983**, *153*, 169−173.
(29) Browne, J. P.; Strom, M.; Martin, S. R.; Bayley, P. M. *Biochemistry* **1997**, *36*, 9550−9561.
(30) Masino, L.; Martin, S. R.; Bayley, P. M. *Protein Sci.* **2000**, *9*, 1519−1529.
(31) Martin, S. R.; Bayley, P. M. *Biochem. J.* **1986**, *238*, 485−490.